

Pulsed-Laser Melting of Amorphous Silicon: Time-Resolved Measurements and Model Calculations

D. H. Lowndes, R. F. Wood, and J. Narayan

Solid State Division, Oak Ridge National Laboratory, Oak Ridge, Tennessee 37831

(Received 23 August 1983)

It is demonstrated that the thermal conductivity of self-ion-implanted, amorphized silicon is an order of magnitude less than that of crystalline silicon and is by far the dominant parameter determining the dynamical response of the ion-implanted silicon system to pulsed-laser radiation; the latent heat and melting temperature of amorphous silicon are relatively unimportant. Transmission electron microscopy indicates that bulk nucleation occurs in the highly undercooled liquid phase; a model simulating this effect is presented.

PACS numbers: 64.70.Dv, 44.60.+k, 66.70.+f, 79.20.Ds

In this Letter we report the results of time-resolved reflectivity measurements and model calculations which, together with transmission electron micrographs, allow us to study the transformation of amorphous (*a*) silicon to the undercooled liquid (*l*) phase and the subsequent resolidification process. The time-resolved measurements employ both a recently developed¹ method for measuring the time of the onset of melting, t_m , during an ~ 18 -nsec (full width at half maximum) heating laser pulse, and the older^{1,2} method of measuring the duration, τ_s , of the high-reflectivity phase (HRP) associated with surface melting. The measured variations in t_m and τ_s with the incident pulsed-laser energy density, E_i , yield detailed information about surface melting that serves as a guide for model calculations. The transmission electron microscopy results indicate that bulk nucleation occurs in the undercooled liquid and thus provide further information for the modeling. With major features of the model established, calculations that differ only in the values assumed for thermal or optical properties of the irradiated material can be used to determine the sensitivity of the melting dynamics to the model parameters. The t_m measurements and transmission electron microscopy results provide particularly powerful constraints in constructing the model and in fixing the value of the thermal conductivity, K_a , of *a*-Si.

One of the principal results of our work is a demonstration of the dominant role played by the low value of K_a in determining both the melting-threshold value of E_i and the subsequent solidification behavior of partially molten layers of *a*-Si, at higher E_i . Our results show that the dynamics of melting and resolidification are relatively insensitive to the values of the melting temperature, T_a , and latent heat, L_a , of *a*-Si. This result is particularly significant in light of apparently conflicting conclusions regarding T_a

obtained by several groups.³⁻⁷

A frequency-doubled Nd laser followed by four dichroic mirrors was used to provide a harmonically pure 532-nm beam with (18 ± 1) -nsec pulse duration. The laser was operated at fixed amplifier gain to avoid slight gain-dependent changes of second-harmonic pulse width; E_i was varied with lenses; a beam splitter was used for *in-situ* monitoring of the energy of every laser shot; a separate vacuum planar photodiode and storage oscilloscope were used to monitor the temporal shape of each pulse. Only laser pulse shapes that were temporally nearly Gaussian were used in the analyses. A cw HeNe probe laser beam, incident at 10° to the sample normal and focused to a $35\text{-}\mu\text{m}$ -diam ($1/e$) spot, a silicon avalanche photodiode detector, and a storage oscilloscope (time constant ~ 1 nsec) were used to monitor the time-resolved reflectivity, R . The *a*-Si layers were produced by implantation of 40-keV Si ions at a dose of $6 \times 10^{15}/\text{cm}^2$ into (100) *n*-type silicon of 1–5 Ω cm resistivity; the transmission electron microscopy showed the amorphous layer to be slightly greater than 1000 \AA thick.

Figure 1 shows results for t_m as a function of E_i ; the data for *c*-Si were taken from Ref. 1. These data were obtained by simultaneously monitoring the time evolution of the R signal and of the incident 532-nm laser pulse and determining t_m during the incident laser pulse. To further reduce errors due to slight variations in pulse shape, the zero of time for these measurements was taken to be the center of the incident laser pulse; *positive* times correspond to melting *before* the peak of the pulse. The experimental t_m is defined as the time when the HRP is first reached. As is expected intuitively, *c*-Si melts only during the latter half of the laser pulse at low E_i , with t_m moving to the front of the laser pulse with increasing E_i (Fig. 1). t_m for *a*-Si exhibits a similar qualitative dependence on E_i but

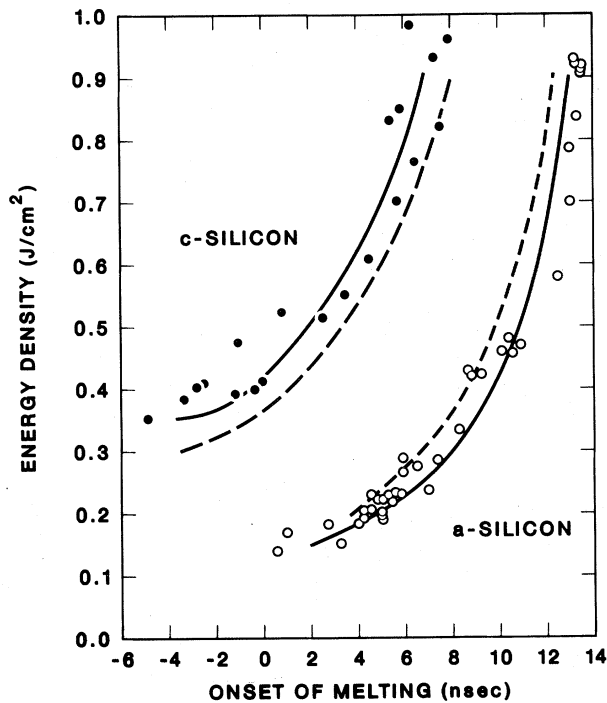


FIG. 1. Measured time of onset of melting (t_m) for α -Si (circles) and for c -Si (dots) vs E_i . Also shown are the results of model calculations of t_m for c - and α -Si (see text).

α -Si, in contrast to c -Si, is never observed to melt as late as the peak of the laser pulse. In fact, for $E_i > 0.6$ J/cm², α -Si melts within the first few nanoseconds of the laser pulse, some 12–13 nsec prior to its peak.

Figure 2 shows the results of our measurements of τ_s vs E_i for α -Si. Also shown for comparison are results of recent τ_s measurements, under nearly identical conditions, for c -Si.¹ The most apparent differences between the two sets of results are that (i) α -Si melts at a significantly lower value of E_i (~ 0.15 J/cm²) than does c -Si ($E_i = 0.35$ J/cm²), and (ii) τ_s for α -Si displays a quasiplateau from ~ 0.25 to ~ 0.4 J/cm².

For c -Si, we recently found that melting-model calculations of τ_s and t_m are quite sensitive, near the melting threshold, to the values used for the optical and thermal properties of c -Si.¹ This result provides confidence that the process may be inverted, i.e., that the observed behavior of t_m vs E_i may be used as a constraint in order to infer thermophysical or optical properties of interest for α -Si; we now demonstrate that this is indeed the case.

The optical properties of α -Si at the wavelength and intensities used in the experiments appear

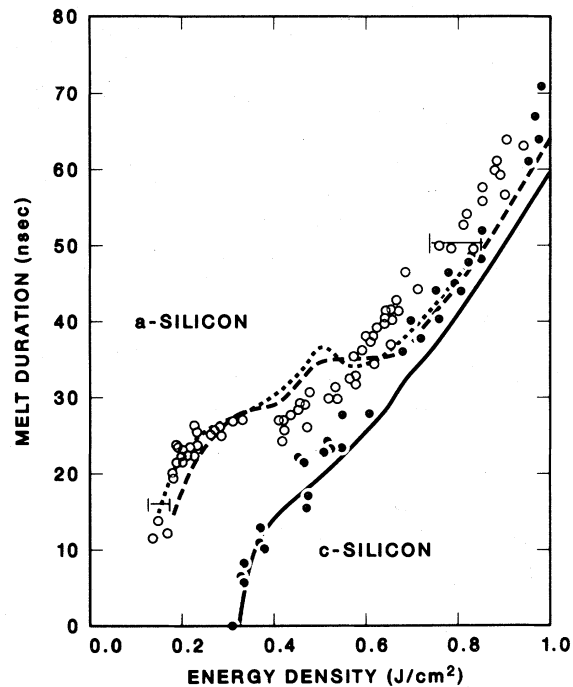


FIG. 2. Measured duration of the high-reflectivity phase (surface melt duration, τ_s) for α -Si (circles) and for c -Si (dots) vs E_i . The error bars are derived from the measured rms precision of the E_i calibrations. Also shown are the results of model calculations of τ_s for α -Si (see text).

not to differ significantly from those used in the calculations of Ref. 1. We used a reflectivity $R_a = 0.42$ and absorption coefficient $\alpha = 5 \times 10^5$ cm⁻¹, independent of T in the solid⁸; on melting of the first cell (~ 100 Å) in the finite-difference calculations, R is increased to 70% and α to 10^6 cm⁻¹. Exploratory calculations were made with many different values of L_a and T_a of α -Si, but our baseline calculations assumed $L_a = 1320$ J/g and $T_a = 1150$ °C, in close agreement with the recent results of Donovan *et al.*⁹ The thermal conductivities K_c and K_l , for c - and l -Si, were obtained as in Ref. 1.

The initial calculations assumed that K_a of α -Si was constant with T and equal to the high-temperature crystalline value, $K_c \approx 0.25$ W/cm-K,¹⁰ but our earliest measurements of t_m showed that this assumption could not be correct. K_a was then successively halved until it was in the range 0.01–0.03 W/cm-K, whereupon satisfactory agreement with experiment was finally obtained. In the calculations described below, we took $K_a = 0.02$ W/cm-K unless otherwise stated; this val-

ue represents an average over the weakly T -dependent $K_a(T)$ expected for an amorphous semiconductor between 300 K and T_a . The agreement that can be obtained between experiment and calculations of t_m vs E_l is shown in Fig. 1 by the two solid curves falling within or close to the measured data for a -Si and c -Si. The dashed curve in the c -Si region shows the results of calculations in which we took $T_a = 1150^\circ\text{C}$ and $L_a = 1320$ J/g, but put $K_a = K_c$. It is apparent that the reduction of L_a and T_a from the corresponding crystalline values ($L_c = 1799$ J/g and $T_c = 1410^\circ\text{C}$) has a relatively minor effect on $t_m(E_l)$. As another example, the dashed curve in the a -Si region of Fig. 1 was obtained by putting $T_a = T_c = 1410^\circ\text{C}$ and $L_a = 1320$ J/g, and keeping $K_a = 0.02$ W/cm-K. These results provide convincing evidence for the dominant role of K_a in determining t_m .

The value $K_a \approx 0.02$ W/cm-K established here for implantation-amorphized Si is quite reasonable. Goldsmid, Kaila, and Paul¹¹ recently obtained the value $K_a(293\text{ K}) = 0.026$ W/cm-K for a 1.15- μm -thick deposited film of a -Si on sapphire, while an estimate of the lattice thermal conductivity, using a Debye phonon spectrum for a -Si, gives $K_a(300\text{ K}) = 0.011$ W/cm-K.

Calculations of the type discussed in Ref. 1 should be adequate for determining the onset of melting, t_m , but it is not clear that they can be modified to describe subsequent solidification from a highly undercooled melt. More specifically, such calculations in the past have generally assumed that the material gives up latent heat at the same temperature at which it is absorbed. In the case of an a -Si layer with $T_a = 1150^\circ\text{C}$, the material would have to cool to 1150°C before solidifying. This is an unnecessarily restrictive condition which, if valid, would seem to imply from thermodynamic considerations that the material could only resolidify as a -Si. However, typical transmission electron micrographs show that if the melt front does not penetrate the a -Si layer, fine-grained polycrystalline Si is formed, followed by a region of large-grained material extending to the front surface; this is an important result whose implications will be discussed at a later time. This suggests, and we will assume it to be the case, that the fine-grained material marks a region in which homogeneous bulk nucleation has occurred at some $T < T_n$, the nucleation temperature, lying between T_a and T_c . The volumetric release of latent heat on bulk nucleation of the c phase is accompanied by either

a very rapid solidification or the creation of a "slush" zone^{12, 13} from which solidification subsequently proceeds at a rapid rate; during this time it may be that no well defined melt front exists. Nucleation does not occur (or occurs very slowly) in the molten Si with $T > T_n$, until a melt front is reestablished at the interface with the fine-grained material.

With the foregoing in mind, the calculations were modified from those of Ref. 1 to include not only the presence of the a -Si layer but also a *simulation* of the effects of bulk nucleation. We emphasize that only one physical and mathematical model of an a -Si layer on a c -Si substrate was used in all of the calculations discussed in this paper. We discussed the results for t_m before considering the need to include undercooling and bulk nucleation in the model only because these two effects are not expected to have any significant influence on t_m , whereas they may greatly influence τ_s . While the melt front is still advancing into the a -Si layer, L_a , T_a , and K_a , K_c , or K_l are used depending on the phase of the material in a given finite-difference cell. The latent heat is always switched from L_a to L_c as soon as an a -Si cell has melted; this is the simplest assumption consistent with the transmission electron microscopy observations. If the melt front does not penetrate to the a - c interface, a layer of a -Si with its low thermal conductivity remains. The l -Si in a given cell is allowed to solidify at the temperature of that cell, provided that this T is less than T_n and that the melt front has begun to recede from its point of maximum penetration. For those molten cells in which T is initially $> T_n$ but $< T_c$, crystallization cannot occur until T drops below T_n or until the rapidly growing region of fine-grained Si can provide nucleation sites for the liquid with $T > T_n$. When the melt front initially contacts the a - c interface, the temperature of the interface, T_{ac} , will be T_a . The melt front cannot penetrate further until T_{ac} rises to T_c and enough latent heat is supplied to begin to melt the c -Si region. If E_l is not great enough for T_{ac} to reach T_c , crystallization will occur at temperatures between T_a and T_c . A thin layer of fine-grained Si may be formed if $T_{ac} < T_n$ but otherwise only large-grained c -Si will be formed. Finally, when $T_{ac} \geq T_c$, epitaxial regrowth of single-crystal Si from the c -Si substrate can proceed just as it would for an entirely c -Si sample.

The results of the calculations of τ_s are shown in Fig. 2. The solid curve in the c -Si region was

taken from Ref. 1 and demonstrates that acceptable agreement can be obtained with the experimental τ_s for *c*-Si. The origin of the apparent displacement of the calculated curve from the experimental points at higher values of E_i is not clear at this time (however, note the experimental error bars). The short-dashed curve in the *a*-Si region was obtained from calculations with $T_a = 1150^\circ\text{C}$, $L_a = 1320\text{ J/g}$, and $K_a = 0.02\text{ W/cm-K}$, while the long-dashed curve used the same values of L_a and K_a but $T_a = T_c = 1410^\circ\text{C}$. Both curves give reasonably good agreement with experiment, given the experimental error bars; thus, a choice between the two sets of parameters is not obvious. In fact, a series of calculations in which T_a was gradually increased to T_c simply gave a family of curves lying between the two shown. Since all of these pairs of T_a , L_a values also give satisfactory agreement with the $t_m(E_i)$ curves of Fig. 1, we again see that it is K_a , not T_a or L_a , which strongly influences the results. The peak in the short-dashed curve at 0.5 J/cm^2 may be an artifact of the present modeling; however, both the calculations and TEM results show that this is approximately the value of E_i for which the melt front contacts the *a-c* interface.

In summary, we have measured the time of onset of melting and the duration of surface melting of a $\sim 1000\text{-\AA}$ -thick layer of *a*-Si formed in *c*-Si by self-ion implantation. Transmission electron microscopy results suggest that bulk nucleation of *c*-Si in the highly undercooled *l*-Si is important, and melting-model calculations were modified to simulate this effect. The calculations establish that the observed onset of melting of *a*-Si at very low energy densities, as well as the measured times of onset of melting versus energy density, can only be explained by an order-of-magnitude decrease in the thermal conductivity of *a*-Si, from the *c*-Si value, to a value $K_a \approx 0.02\text{ W/cm-K}$. Neither the onset of melting nor the duration of surface melting are particularly sensitive to the melting temperature or latent heat of

a-Si.

This research was sponsored by the Division of Materials Sciences, U. S. Department of Energy under Contract No. W-7405-eng-26 with the Union Carbide Corporation.

¹D. H. Lowndes, R. F. Wood, and R. D. Westbrook, *Appl. Phys. Lett.* **43**, 258 (1983).

²D. H. Auston, J. A. Golovchenko, A. L. Simons, R. E. Slusher, P. R. Smith, C. M. Surko, and T. N. C. Venkatesan, in *Laser-Solid Interactions and Laser Processing—1978*, edited by S. D. Ferris, H. J. Leamy, and J. M. Poate, AIP Conference Proceedings No. 50 (American Institute of Physics, New York, 1979).

³G. L. Olson, S. A. Kokorowski, J. A. Roth, and L. D. Hess, in *Laser-Solid Interactions and Transient Thermal Processing of Materials*, edited by J. Narayan, W. L. Brown, and R. Lemons (North-Holland, New York), p. 141, and references herein to earlier papers by these authors.

⁴B. G. Bagley and H. S. Chen, in *Laser-Solid Interactions and Laser Processing—1978*, edited by S. D. Ferris, H. J. Leamy, and J. M. Poate, AIP Conference Proceedings No. 50 (American Institute of Physics, New York, 1979), p. 97.

⁵F. Spaepen and D. Turnbull, in *Laser-Solid Interactions and Laser Processing—1978*, edited by S. D. Ferris, H. J. Leamy, and J. M. Poate, AIP Conference Proceedings No. 50 (American Institute of Physics, New York, 1979), p. 73.

⁶P. Baeri, G. Foti, J. M. Poate, and A. G. Cullis, *Phys. Rev. Lett.* **45**, 2036 (1980).

⁷J. A. Knapp and S. T. Picraux, *Appl. Phys. Lett.* **38**, 873 (1981).

⁸G. E. Jellison, Jr., private communication.

⁹E. P. Donovan, F. Spaepen, D. Turnbull, J. M. Poate, and D. C. Jacobson, *Appl. Phys. Lett.* **42**, 698 (1983).

¹⁰C. J. Glassbrenner and G. A. Slack, *Phys. Rev.* **134**, A1058 (1964).

¹¹H. J. Goldsmid, M. M. Kaila, and G. L. Paul, *Phys. Status Solidi A* **76**, K31 (1983).

¹²R. F. Wood and G. E. Giles, *Phys. Rev. B* **23**, 2923 (1981).

¹³R. F. Wood, to be published.